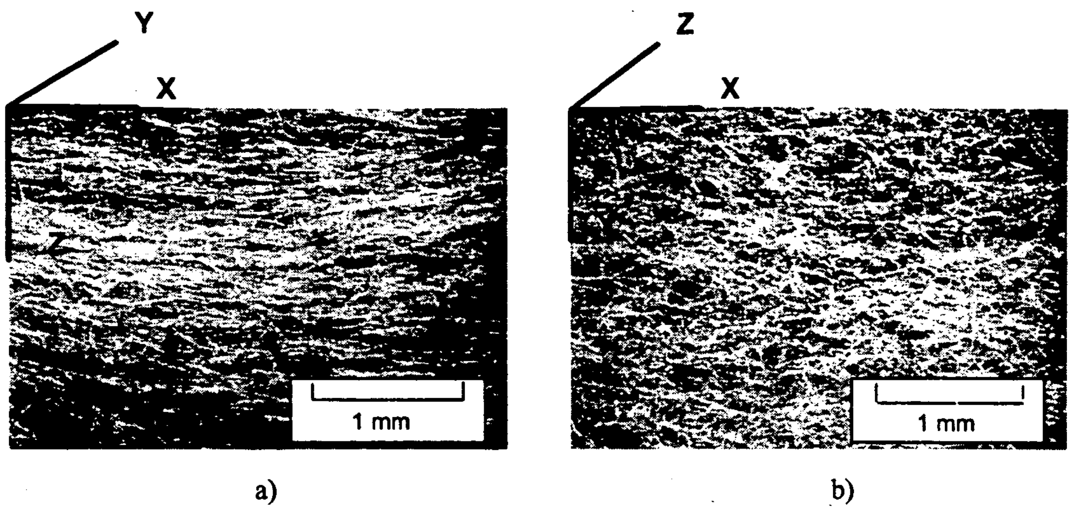

Fig. 1 Configuration of Kevlar 29 unidirectional webbing material.
a) Side view of webbing sheet (**ZX** plane), b) Top view of web sheet (**YX** plane, where **X** is the direction of carding machine and conveyor belt.

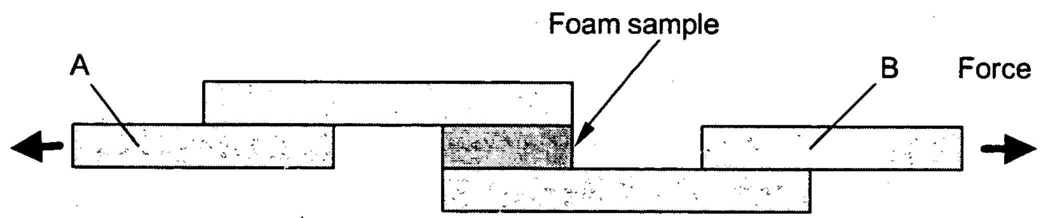

Fig. 2 Schematic of shear test fixture following ASTM C 273. Steel plates A and B are attached to a foam sample of equal thickness (6 mm), and exert a shear force.

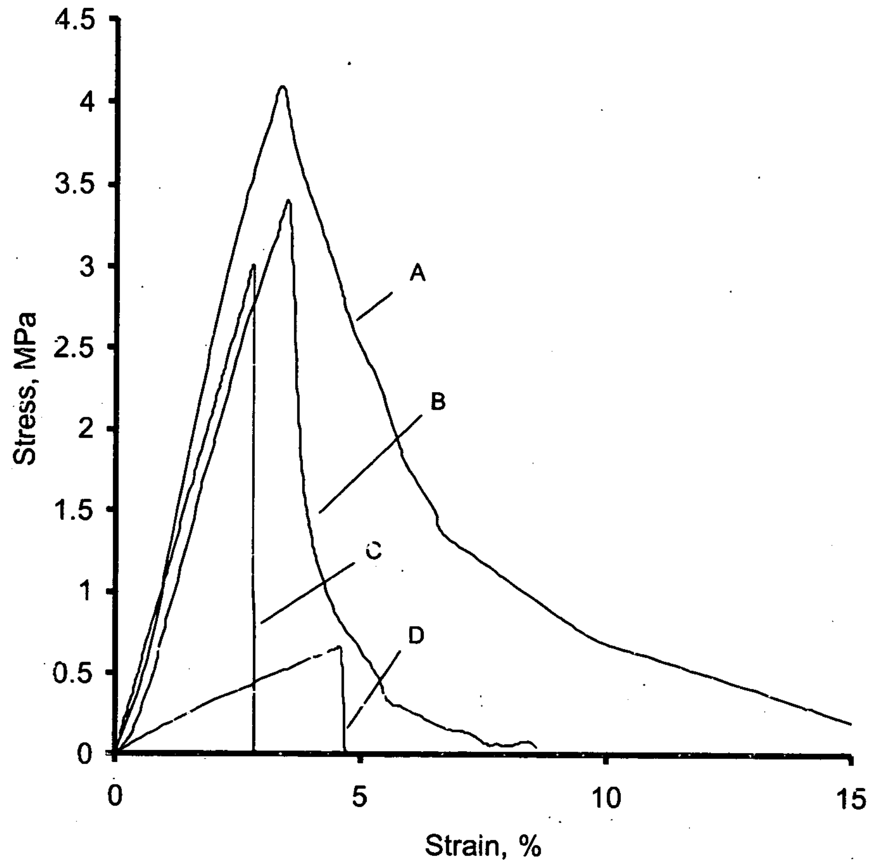

Fig. 3 Tensile stress-strain plot for PVC foam samples with density = 100 kg / m^3:

a) Foam reinforced with 10 wt % aramid fibers treated with 3 wt % phenolic resin,

b) Foam reinforced with 4 wt % aramid fibers treated with 1.2 wt % phenolic resin,
c) Cross-linked commercial PVC foam, d) Unreinforced PVC foam based on microspheres.

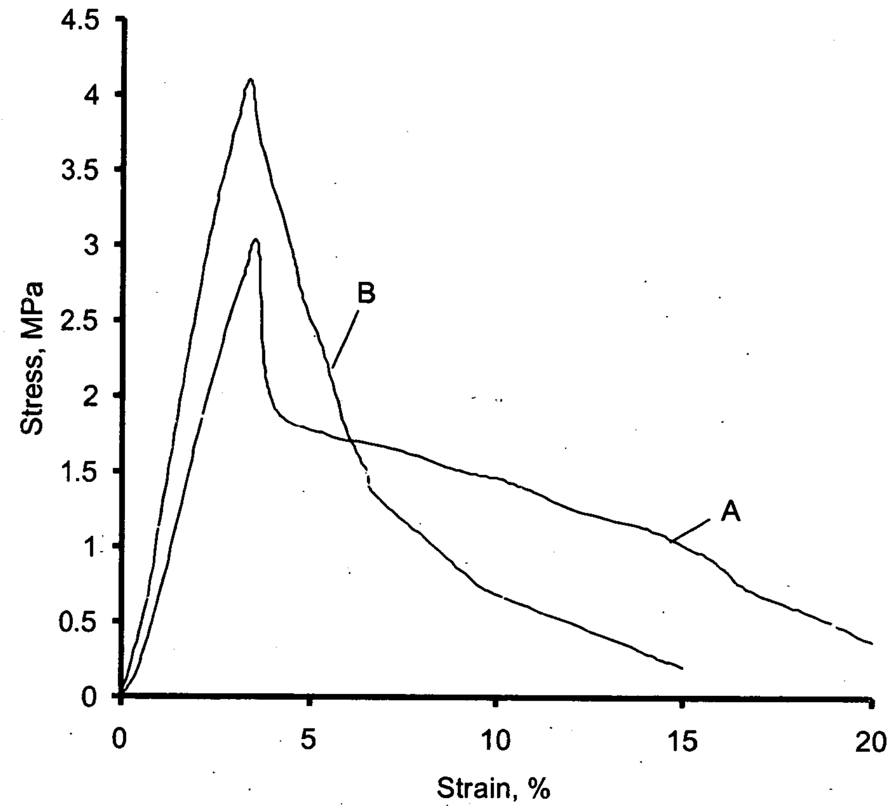

Fig. 4 Tensile stress–strain plot for PVC composite foam reinforced with 10 wt% fiber webbing treated with 0.4 wt% phenolic (curve A), and 3 wt% phenolic (curve B).

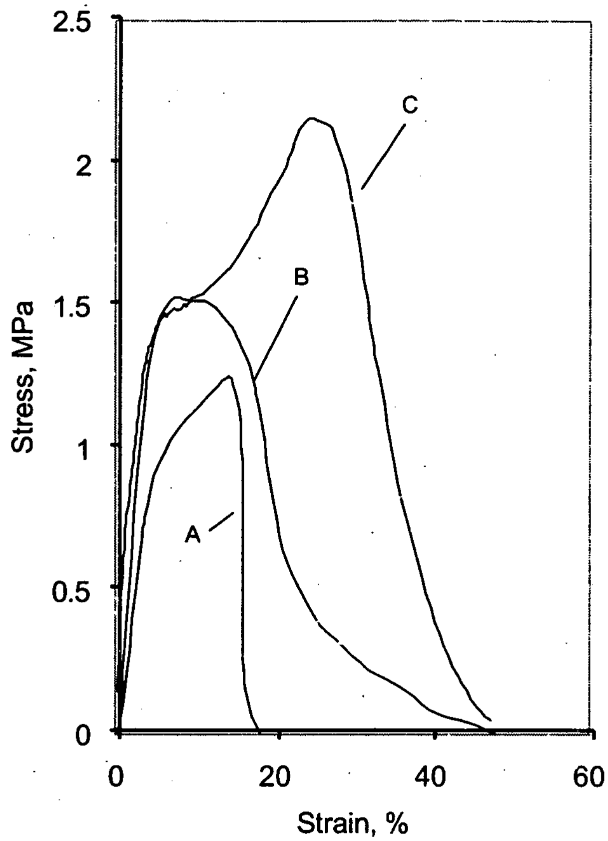

Fig. 5 Shear stress–strain curves for foam samples with density = 100 kg / cm^3, including unreinforced foam based on PVC microspheres (curve A), cross-linked commercial PVC foam (curve B), and PVC composite foam PVC (10 wt % fibers, 3 wt % phenolic), with fibers perpendicular to the shear plane (curve C).

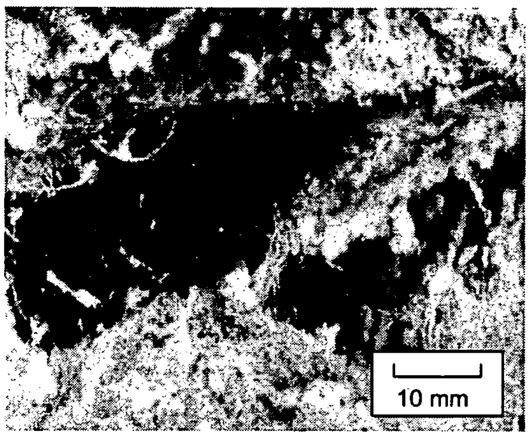

a)

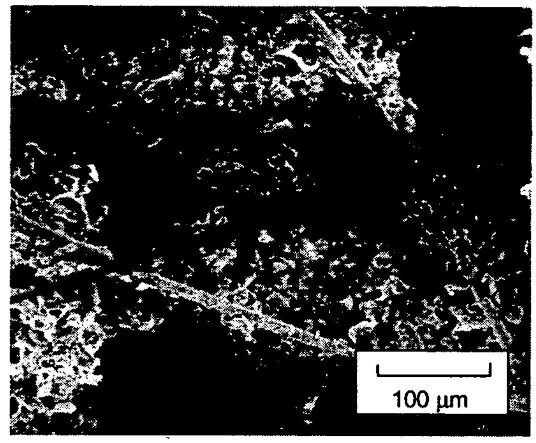

b)

Fig. 6 Cracks in shear-tested composite PVC foam (10 wt % aramid fibers, 3 wt % phenolic resin). a) Crack region showing fiber bridging. b) Crack region showing fibers well-bonded to PVC microspheres.

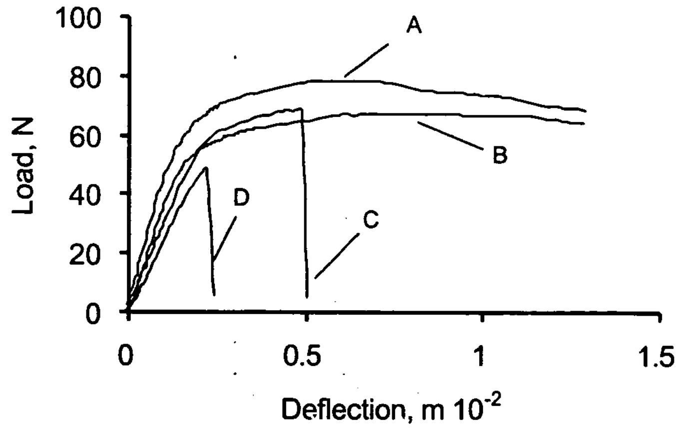

a)

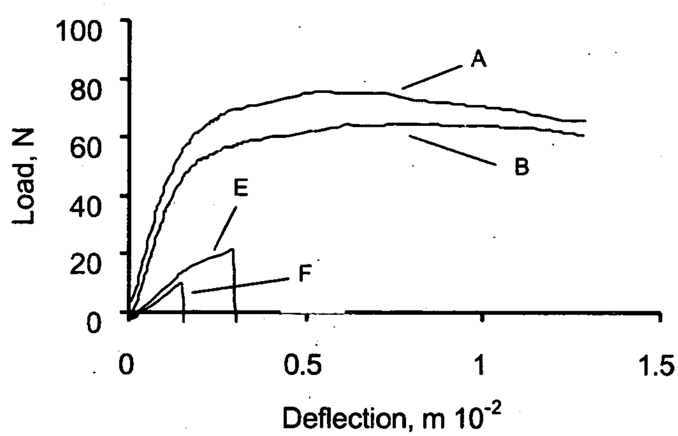

b)

Fig. 7 Load-deflection data from flexural tests for foam materials with density = 100 kg / m^3. a) compares un-notched and notched beams of PVC composite foam (curves A and B) with un-notched and notched beams of cross-linked commercial PVC foam (curves C and D) respectively b) compares un-notched and notched beams of PVC composite foam (curves A and B) with un-notched and notched beams with un-notched and notched foam made from PVC microspheres (curves E and F) respectively.

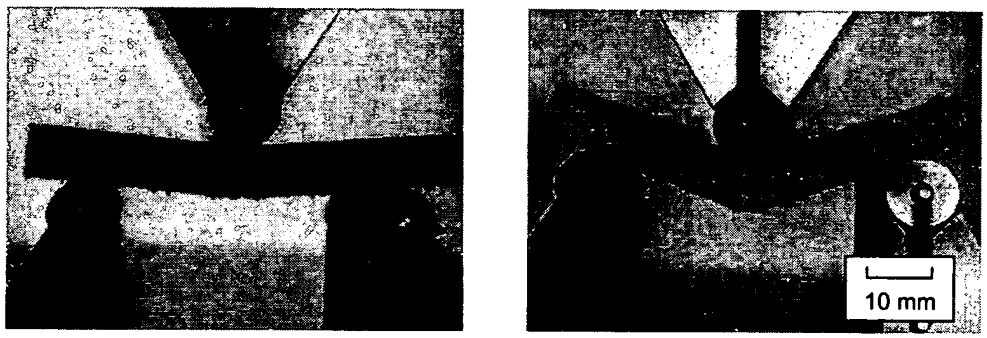

a) b)

Fig. 8 Crack resistance of notched foam samples. a) Cross-linked PVC foam at 2.5 mm deflection with zero load capacity. b) Composite foam (10 wt % fiber, 3 wt % phenolic) at 14 mm deflection and 60 N load. Beams correspond to load-deflection data shown in Figure 7.

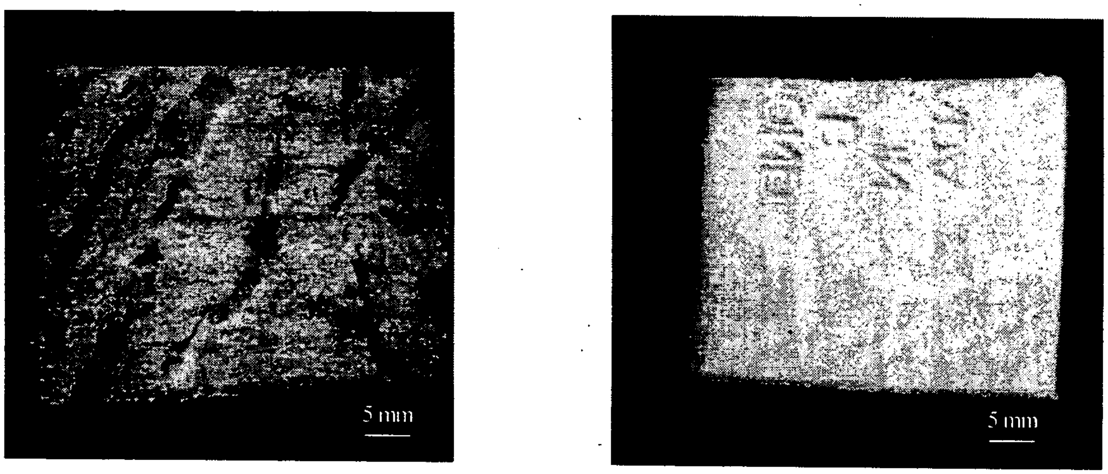

a) b)

FIG. 9

Foam produced using unexpanded microspheres only (a), and foam using a 7:1 mixture of expanded and unexpended microspheres (b).

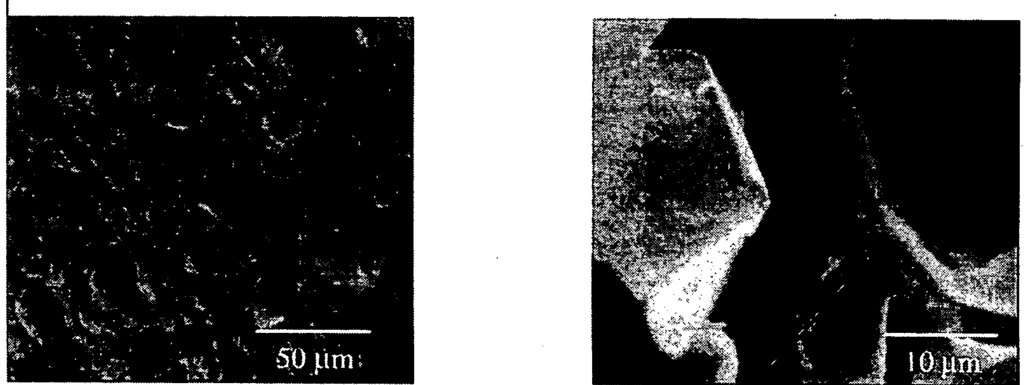

a) b)

Triple junctions of the cell walls

FIG. 10

SEM images of neat foam sample prepared improved process conditions:
a) global view, and b) enlarged region showing triple junction.

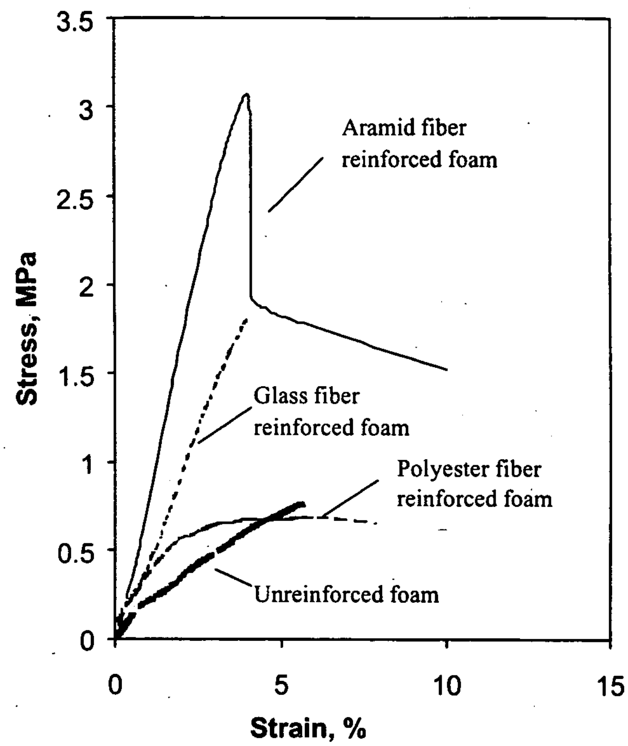

FIG. 11

Tensile stress-strain plot for foam samples based on PAN microspheres. a) Unreinforced foam with density = 100 kg / m^3. b) Foam reinforced with long polyester fiber batt (density = 100 kg / m^3 , fiber weight percent = 30. c) Foam reinforced with long glass fiber batt (density = 100 kg / m^3 , fiber weight percent = 8). d) Foam reinforced with long aramid fiber batt (density = 100 kg / m^3 and fiber weight percent = 8).

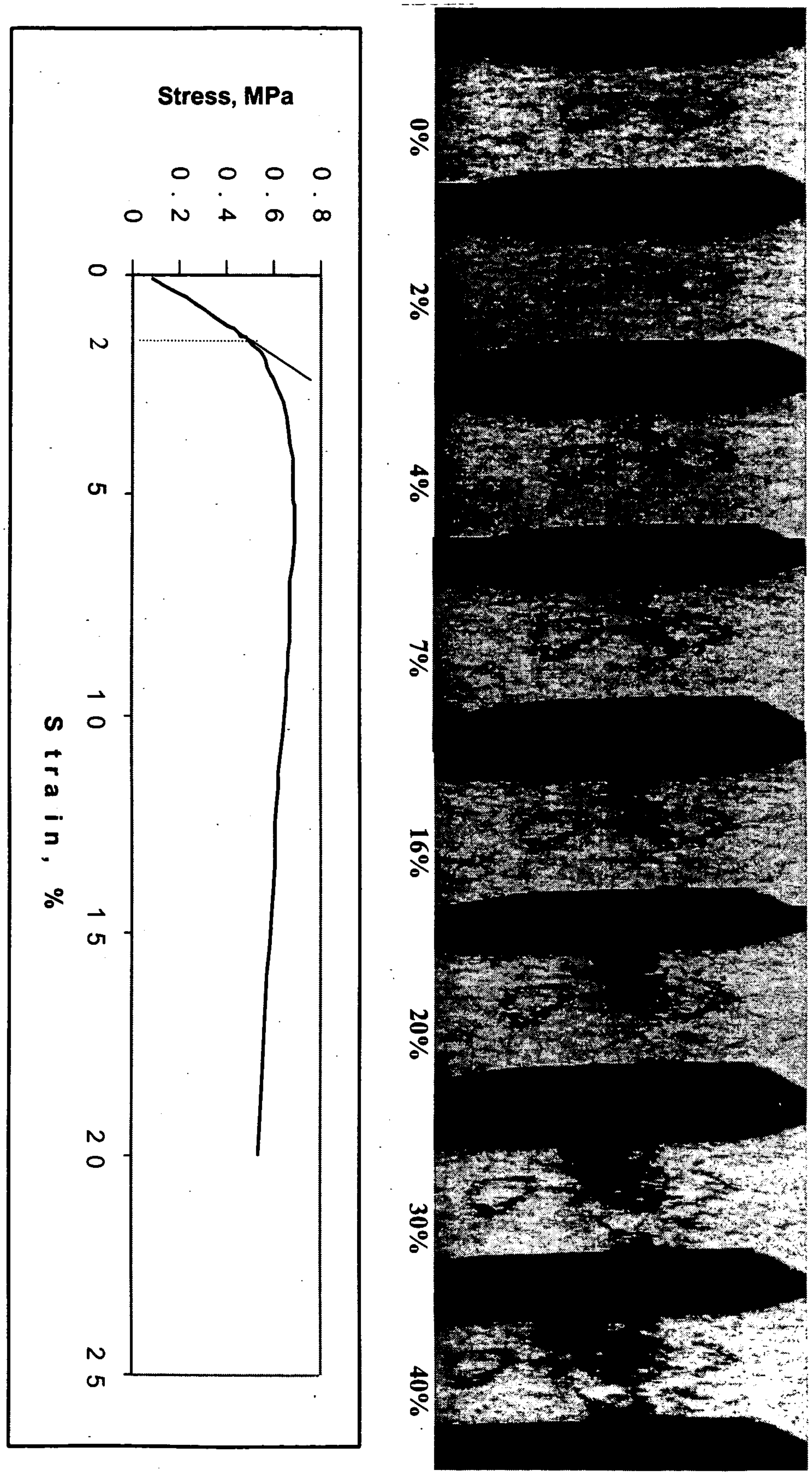

Long-term crack propagation during tensile testing of polyester fiber reinforced foam.

FIG. 12

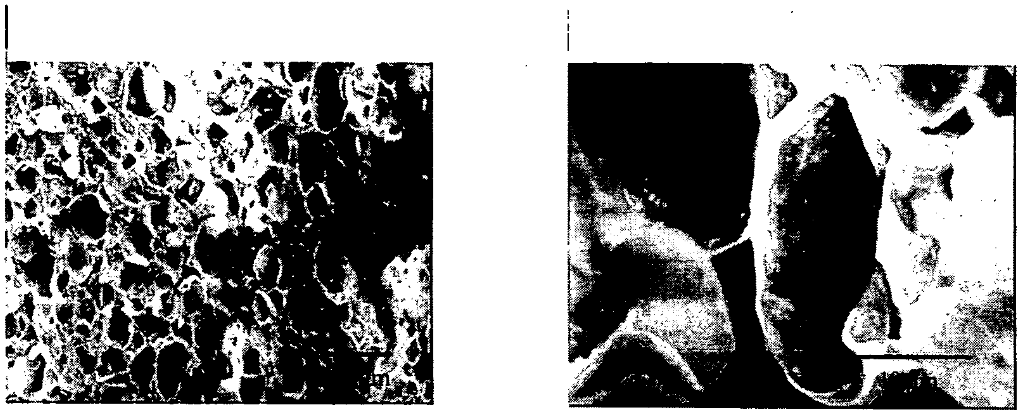

a) b)

FIG. 13

SEM images of fractured tensile samples of neat foam. The enlargement in (b) shows torn microspheres.

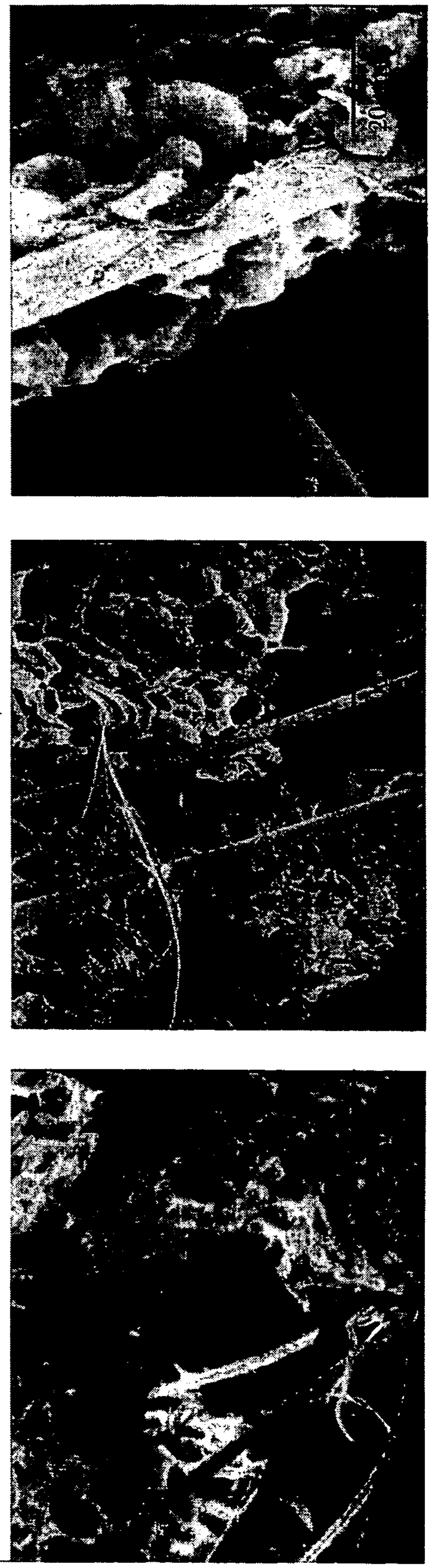

a) b) c)

Tensile fracture surface of aramid fiber reinforced PAN foam sample: a) segments of fibers protruding from the foam indicate crack bridging, b) broken fibrillated fiber segment, and c) fiber segment with bonded microspheres.

FIG. 14

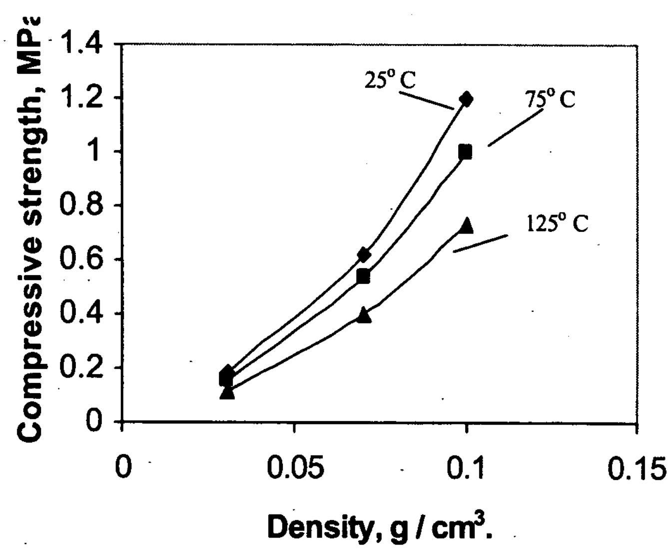

FIG. 15

Compressive strength of neat foam versus of foam density for different test temperatures

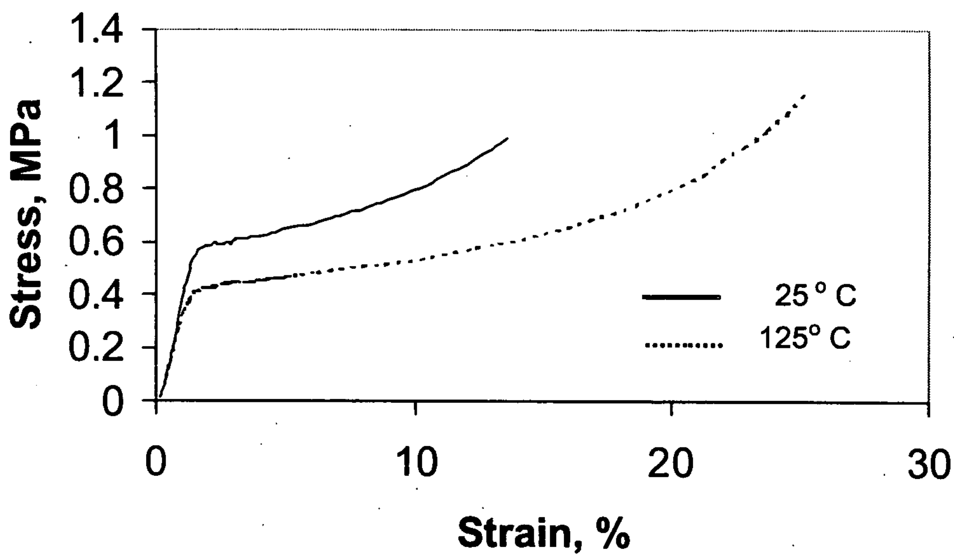

FIG. 16

Compressive strain - stress plots at different temperatures for unreinforced foam with density 70 kg / m^3 (4.4 pcf)

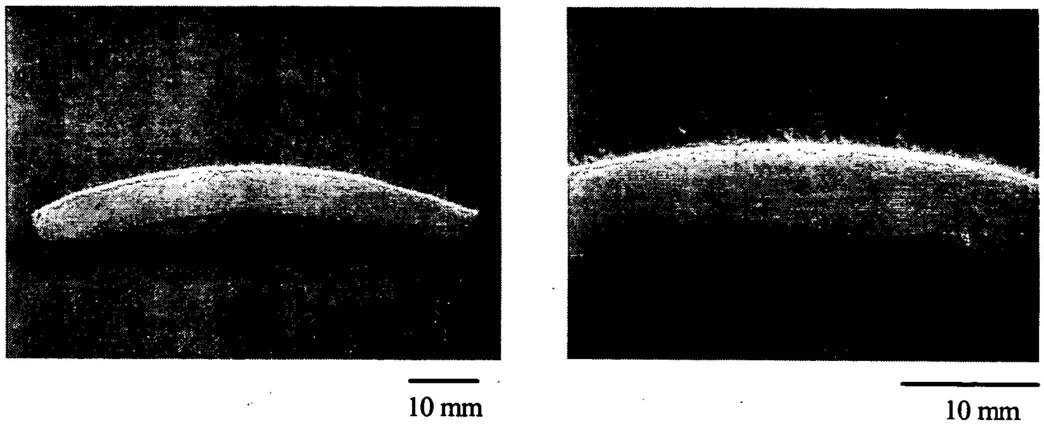

a) b)

Demonstration of formability of aramid fiber reinforced PAN foam: a) sample hot-formed from flat plate, and b) enlargement showing absence of forming-induced defects.

FIG. 17